Physics Letters B 732 (2014) 41–48

Contents lists available at ScienceDirect

Physics Letters B

www.elsevier.com/locate/physletb

Nucleon axial charge and pion decay constant from two-flavor lattice QCD

R. Horsley [a], Y. Nakamura [b], A. Nobile [c], P.E.L. Rakow [d], G. Schierholz [e,*], J.M. Zanotti [f]

[a] School of Physics and Astronomy, University of Edinburgh, Edinburgh EH9 3JZ, United Kingdom
[b] RIKEN Advanced Institute for Computational Science, Kobe, Hyogo 650-0047, Japan
[c] JSC, Forschungszentrum Jülich, 52425 Jülich, Germany
[d] Theoretical Physics Division, Department of Mathematical Sciences, University of Liverpool, Liverpool L69 3BX, United Kingdom
[e] Deutsches Elektronen-Synchrotron DESY, 22603 Hamburg, Germany
[f] CSSM, School of Chemistry and Physics, University of Adelaide, Adelaide SA 5005, Australia

ARTICLE INFO

Article history:
Received 8 January 2014
Received in revised form 18 February 2014
Accepted 1 March 2014
Available online 7 March 2014
Editor: A. Ringwald

ABSTRACT

The axial charge of the nucleon g_A and the pion decay constant f_π are computed in two-flavor lattice QCD. The simulations are carried out on lattices of various volumes and lattice spacings. Results are reported for pion masses as low as $m_\pi = 130$ MeV. Both quantities, g_A and f_π, suffer from large finite size effects, which to leading order ChEFT and ChPT turn out to be identical. By considering the naturally renormalized ratio g_A/f_π, we observe a universal behavior as a function of decreasing quark mass. From extrapolating the ratio to the physical point, we find $g_A^R = 1.29(5)(3)$, using the physical value of f_π as input and $r_0 = 0.50(1)$ to set the scale. In a subsequent calculation we attempt to extrapolate g_A and f_π separately to the infinite volume. Both volume and quark mass dependencies of g_A and f_π are found to be well described by ChEFT and ChPT. We find at the physical point $g_A^R = 1.24(4)$ and $f_\pi^R = 89.6(1.1)(1.8)$ MeV. Both sets of results are in good agreement with experiment. As a by-product we obtain the low-energy constant $\bar{l}_4 = 4.2(1)$.

1. Introduction

The axial charge g_A of the nucleon is a fundamental measure of nucleon structure. While g_A has been known accurately for many years from neutron β decays, a calculation of g_A from first principles still presents a significant challenge. Present lattice calculations [1–5], except perhaps Ref. [4], underestimate the experimental value by a large amount. The resolution of this problem is of great importance to any further calculation of hadron structure.

Lattice calculations of g_A are in many ways connected to calculations of the pion decay constant f_π. Both quantities involve the axial vector current, which is not conserved and thus needs to be renormalized. Though it is standard practice nowadays to compute the renormalization constant nonperturbatively (see, for example, [6,7]), some scope of uncertainty remains [8]. Another common feature is that g_A and f_π seem to be affected by large finite size corrections, in particular at small pion masses, which to leading order ChEFT and ChPT [9–11] appear to be the same in both cases. This led us to suggest to determine g_A from the ratio g_A/f_π. Preliminary results [12] were encouraging, and we present here the final analysis of this investigation.

The calculations are done with two flavors of nonperturbatively $O(a)$ improved Wilson fermions and Wilson plaquette action [13], including simulations at virtually physical pion mass and on a variety of lattice volumes. This allows for a separate extrapolation of both g_A and f_π to the infinite volume and the physical point.

2. Lattice simulation

Our lattice ensembles are listed in Table 1. The pion masses and the chirally extrapolated values of r_0/a are taken from our preceding paper [13] on the nucleon mass and sigma term. The Sommer parameter was found to be $r_0 = 0.50(1)$ fm, which we will use to set the scale throughout this Letter. The ensembles cover three β values, $\beta = 5.25$, 5.29 and 5.40, with lattice spacings $a = 0.076$, 0.071 and 0.060 fm.

We employ the improved axial vector current

$$\mathcal{A}_\mu(x) = \bar{q}(x)\gamma_\mu\gamma_5 q(x) + ac_A\partial_\mu\bar{q}(x)\gamma_5 q(x), \quad (1)$$

* Corresponding author.

http://dx.doi.org/10.1016/j.physletb.2014.03.002

Table 1
Parameters of our lattice data sets, together with the pion mass, the bare axial charge and the pion decay constant. Also listed are the chirally extrapolated values of r_0/a. In this work we use $r_0 = 0.50(1)$ fm to convert lattice numbers to physical units.

β	κ	Volume	am_π	g_A	af_π	r_0/a
5.25	0.13460	$16^3 \times 32$	0.4932(10)	1.442(13)	0.0886(8)	6.603(53)
5.25	0.13520	$16^3 \times 32$	0.3821(13)	1.438(20)	0.0756(8)	
5.25	0.13575	$24^3 \times 48$	0.2556(5)	1.456(10)	0.0635(5)	
5.25	0.13600	$24^3 \times 48$	0.1840(7)	1.412(18)	0.0550(4)	
5.25	0.13620	$32^3 \times 64$	0.0997(11)	1.368(51)	0.0439(6)	
5.29	0.13400	$16^3 \times 32$	0.5767(11)	1.437(12)	0.0936(9)	7.004(54)
5.29	0.13500	$16^3 \times 32$	0.4206(9)	1.409(12)	0.0778(5)	
5.29	0.13550	$12^3 \times 32$	0.3605(32)	1.181(60)	0.0568(8)	
5.29	0.13550	$16^3 \times 32$	0.3325(14)	1.371(20)	0.0675(6)	
5.29	0.13550	$24^3 \times 48$	0.3270(6)	1.459(11)	0.0689(7)	
5.29	0.13590	$12^3 \times 32$	0.3369(62)	0.967(105)	0.0345(9)	
5.29	0.13590	$16^3 \times 32$	0.2518(15)	1.271(32)	0.0559(5)	
5.29	0.13590	$24^3 \times 48$	0.2395(5)	1.426(7)	0.0588(3)	
5.29	0.13620	$24^3 \times 48$	0.1552(6)	1.334(18)	0.0478(3)	
5.29	0.13632	$24^3 \times 48$	0.1112(9)	1.271(67)	0.0398(4)	
5.29	0.13632	$32^3 \times 64$	0.1070(5)	1.409(24)	0.0440(3)	
5.29	0.13632	$40^3 \times 64$	0.1050(3)	1.439(17)	0.0445(3)	
5.29	0.13640	$40^3 \times 64$	0.0660(8)	1.363(105)	0.0375(5)	
5.29	0.13640	$48^3 \times 64$	0.0570(7)	1.572(52)	0.0408(11)	
5.40	0.13500	$24^3 \times 48$	0.4030(4)	1.474(7)	0.0691(5)	8.285(74)
5.40	0.13560	$24^3 \times 48$	0.3123(7)	1.451(11)	0.0620(5)	
5.40	0.13610	$24^3 \times 48$	0.2208(7)	1.410(20)	0.0513(4)	
5.40	0.13625	$24^3 \times 48$	0.1902(6)	1.377(20)	0.0470(3)	
5.40	0.13640	$24^3 \times 48$	0.1538(10)	1.261(34)	0.0419(4)	
5.40	0.13640	$32^3 \times 64$	0.1505(5)	1.402(17)	0.0442(4)	
5.40	0.13660	$32^3 \times 64$	0.0845(6)	1.206(79)	0.0342(4)	
5.40	0.13660	$48^3 \times 64$	0.0797(3)	1.403(29)	0.0362(3)	

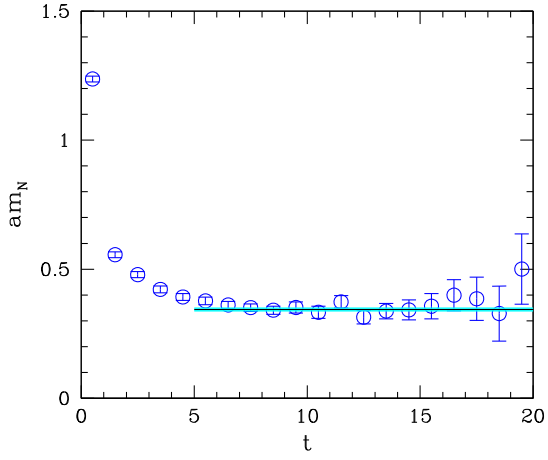

Fig. 1. The effective mass m_N of the nucleon on the 48×64 lattice at $\beta = 5.29$, $\kappa = 0.13640$, corresponding to our smallest pion mass. The horizontal line shows the fit and error band. The fit range for this nucleon mass was $t = 8$–16.

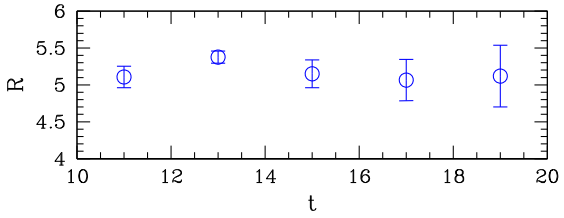

Fig. 2. The ratio R as a function of the source-sink time separation t on the $24^3 \times 48$ lattice at $\beta = 5.29$, $\kappa = 0.13590$.

where c_A is taken from [14]. The improvement term does not contribute to forward matrix elements, but it will contribute to f_π. The calculation of g_A follows [10,15,16] with one exception, namely that on the $48^3 \times 64$ lattice at $\beta = 5.29$, $\kappa = 0.13640$ we have employed Wuppertal smearing instead of Jacobi smearing. It involves computing the ratio of two- and three-point functions

$$R_{\alpha\beta}(t,\tau) = \frac{\langle N_\alpha(t)\mathcal{A}_\mu(\tau)\bar{N}_\beta(0)\rangle}{\langle N(t)\bar{N}(0)\rangle}, \tag{2}$$

$\bar{N}$ and N being the nucleon creation and annihilation operators at zero momentum with Dirac indices α, β, which are used to project onto the appropriate nucleon spin. The spins of the nucleon appearing in the denominator are summed over. Any smearing of the source (at time 0) and sink operators (at time t) is cancelled in this ratio. For $\beta = 5.4$ we use $t = 17$, while the lightest two ensembles at $\beta = 5.29$, $\kappa = 0.13640$ and $\kappa = 0.13632$, use $t = 15$. All other ensembles use $t = 13$. In physical units this amounts to time separations between source and sink of ≈ 1.1 fm at the smaller pion masses, which is current state of the art (see Table 3 of [17]). In Fig. 1 we plot the effective mass m_N of the nucleon at our smallest, nearly physical pion mass, which indicates that excited states have died out at times $t \gtrsim 5$. To determine the nucleon mass on this ensemble, we chose the conservative fit range $t = 8$–16.

In [4] it has been argued that contributions from excited states might be the reason for lattice calculations to underestimate g_A, when compared to its experimental value. To investigate this scenario (beyond tuning the smearing parameters, see Fig. 1), we have performed additional simulations on the $24^3 \times 48$ lattice at $\beta = 5.29$, $\kappa = 0.13590$ with a large range of different source-sink separations, $t = 11, \ldots, 19$ $(0.79, \ldots, 1.36$ fm), albeit with somewhat lower statistics than our reference point at $t = 13$ (0.93 fm) on this ensemble. In Fig. 2 we show the ratio R for various time separations t between source and sink. If our g_A determinations were affected by excited state contaminations, then we should find a larger value at separations $t > 13$. However, we do not see any

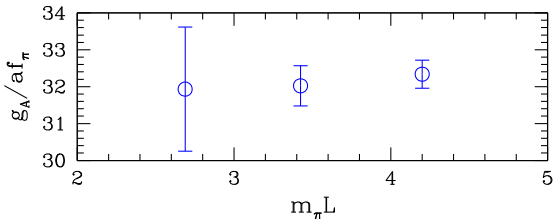

Fig. 3. The ratio $g_A(L)/af_\pi(L)$ as a function of $m_\pi L$ at $\beta = 5.29$, $\kappa = 0.13632$.

systematic deviation of R from our result at $t = 13$ within the error bars, not even for $t = 11$. This provides us with confidence that our choices of t are sufficient with our choice of source and sink smearing. Similar conclusions were found in [3].

Our smearing parameters are tuned to give a *rms* radius of ≈ 0.5 fm, which is about half the radius of the nucleon. For this level of smearing no further improvement of the extracted result for g_A was found by employing variational techniques [17], which systematically separate excited states out from the ground state at source and sink.

The calculation of f_π follows [18]. We use the notation employed in ChPT, with the experimental value $f_{\pi^+} = 92.2$ MeV. Our final results for the bare quantities, g_A and af_π, on all our ensembles, are given in Table 1.

3. Results

Except for the very lowest pion mass, $m_\pi L \gtrsim 4$ (L being the spatial extent of the lattice) on our larger lattices at any other κ value, which is state of the art for pion masses of $O(200)$ MeV. But even on lattices of this size g_A, f_π and m_π are found to suffer from finite size effects, which we have to deal with in one way or another.

Finite size corrections to g_A, f_π and m_π have been studied extensively in the literature. In Appendix A we show, based on predictions of ChEFT and ChPT adapted to the finite volume, that the leading corrections to g_A and f_π are identical and cancel in the ratio g_A/f_π. This makes g_A/f_π the preferred quantity for computing g_A.

3.1. The axial coupling g_A from the ratio $g_A(L)/f_\pi(L)$

Neglecting NNLO and $O(\Delta(L))$ corrections, we obtain from Eqs. (19) and (20)

$$\frac{g_A(L) - g_A(\infty)}{g_A(\infty)} = \frac{f_\pi(L) - f_\pi(\infty)}{f_\pi(\infty)}. \tag{3}$$

Denoting the physical, renormalized axial charge and pion decay constant in the infinite volume by g_A^R and f_π^R, respectively, and making use of the fact that the renormalization constant Z_A of the axial vector current cancels in the ratio g_A/f_π, we then have

$$\frac{g_A^R}{f_\pi^R} = \frac{g_A(\infty)}{f_\pi(\infty)} = \frac{g_A(L)}{f_\pi(L)}. \tag{4}$$

To test this relation, we plot g_A/af_π for three different lattice volumes at our second lowest pion mass in Fig. 3. The ratio is found to be independent of the volume, within the errors, which demonstrates that finite size corrections cancel indeed in g_A/f_π.

Let us now turn to the calculation of g_A. In Fig. 4 we plot the ratio $g_A(L)/f_\pi(L)$ for our (raw) data points listed in Table 1, restricting ourselves to pion masses $m_\pi \leqslant 750$ MeV, and taking $r_0 = 0.50(1)$ fm to set the scale. If we have more than one volume at a given κ value, we show the result of the largest volume. The

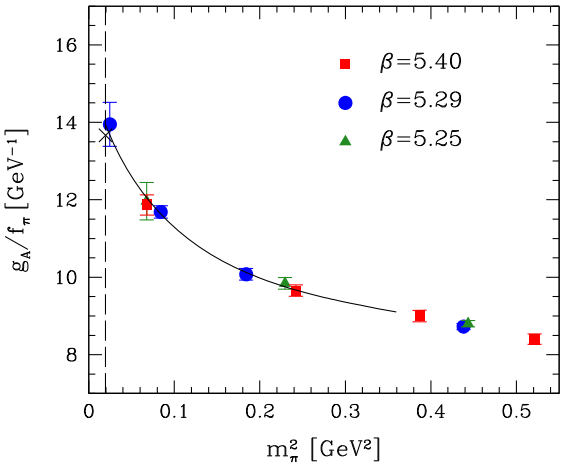

Fig. 4. The ratio $g_A(L)/f_\pi(L)$ as a function of $m_\pi^2(L)$, together with the experimental value ($\times$). The curve shows a fit of Eq. (5) to the data.

lowest pion mass in Fig. 4 is 157 MeV. The data points of all three β values lie nicely on a universal curve. At $m_\pi^2 \approx 0.06$, 0.23 and 0.44 GeV^2, for example, where we have results for more than one lattice spacing, the data points coincide with each other, indicating that discretization effects are negligible.

With finite size corrections being practically absent, the leading order chiral expansion of g_A/f_π can be cast in the form [10,19,20]

$$\frac{g_A}{f_\pi} = A + Bm_\pi^2 + Cm_\pi^2 \ln m_\pi^2 + Dm_\pi^4. \tag{5}$$

We have fitted Eq. (5) to the data points in Fig. 4. The result is shown by the solid curve. At the physical point this gives

$$\frac{g_A}{f_\pi} = 13.95 \pm 0.71 \pm 0.30\ \text{GeV}^{-1}. \tag{6}$$

The second error is due to the error on r_0. Multiplying the ratio (6) by the physical value of f_π, $f_\pi^R = 92.2$ MeV, we then obtain

$$g_A^R = 1.29 \pm 0.05 \pm 0.03. \tag{7}$$

Alternatively, we could have set the scale by the physical value of f_π, using the results of Section 3.2. That would give the value $g_A^R = 1.27(5)$.

Now that we have presented the main result of the Letter, i.e. g_A^R from the ratio $g_A(L)/f_\pi(L)$, we proceed to study g_A^R and f_π^R separately and present results in the context of established expressions from finite volume ChEFT and ChPT.

3.2. g_A and f_π in the infinite volume

We now consider explicitly the finite size formulae as given in Appendix A. In the following fits we take $f_0 = 86$ MeV [21]. There is some freedom in which pion mass to take in Eqs. (19), (20) and (24). We choose $m_\pi = m_\pi(\infty)$ in λ, $\lambda(y)$ and $c(m_\pi)$, and $m_\pi = m_\pi(L)$ otherwise.

Let us first consider the pion mass. In Fig. 5 we show the fits of Eq. (24) to m_π for two of our lattice ensembles. The corrections to m_π are well described by this equation. Apart from $m_\pi(\infty)$, we have one free parameter, $c(m_\pi)$, only. Equally good fits are obtained for $\beta = 5.40$, $\kappa = 0.13660$ and 0.13640. The parameter $c(m_\pi)$ is found to vanish with a large inverse power of the pion mass.[1] The finite size corrections predicted by the NLO expression (21), on the other hand, are nowhere near as big as the effect

[1] At $\beta = 5.29$, $\kappa = 0.13632$, i.e. our second smallest pion mass, $c(m_\pi)$ has dropped to the value 0.15 already.

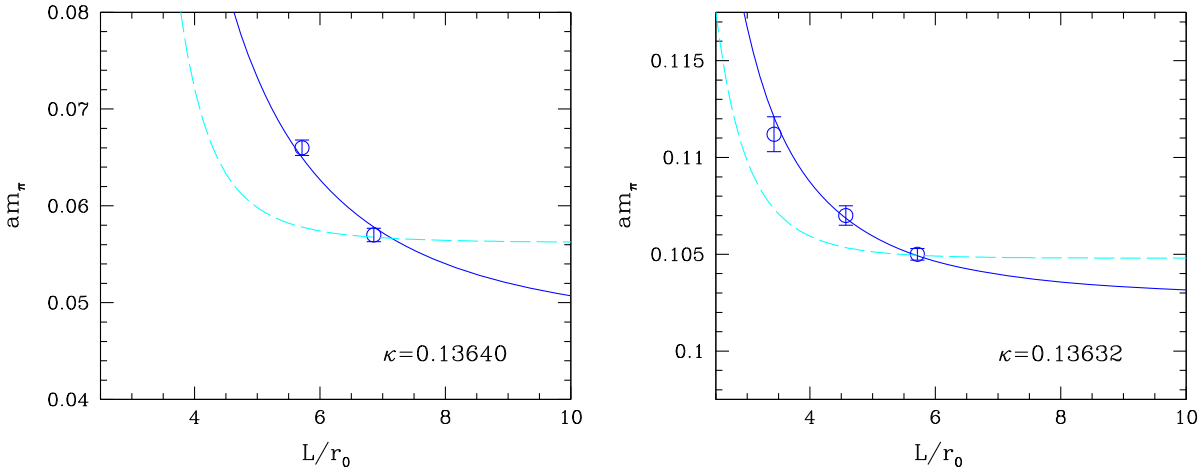

Fig. 5. The pion mass am_π as a function of lattice size for two ensembles at $\beta = 5.29$. The solid line shows a fit of Eq. (24) to the data. The dashed line shows the NLO result, Eq. (21), fitted to the smallest mass point.

Table 2
The pion mass and the renormalized axial coupling and pion decay constant extrapolated to the infinite volume for $m_\pi \leqslant 500$ MeV and $r_0 = 0.50$ fm.

β	κ	m_π [MeV]	g_A^R	f_π^R [MeV]
5.25	0.13600	479(2)	1.07(1)	108.9(0.8)
5.29	0.13620	426(2)	1.05(2)	103.6(0.6)
5.29	0.13632	284(2)	1.10(2)	94.7(0.6)
5.29	0.13640	130(5)	1.24(4)	89.7(1.5)
5.40	0.13640	492(2)	1.09(1)	112.3(0.9)
5.40	0.13660	253(2)	1.09(2)	93.0(0.7)

shown by the data. In Table 2 we list our final pion masses. Our lowest mass turns out to be $m_\pi = 130(5)$ MeV.

Let us now turn to the axial charge and the pion decay constant. In Fig. 6 we show the fits of Eqs. (19) and (20) to g_A and af_π, respectively, for our three lowest pion masses. In this case the fits involve one free parameter each, $g_A(\infty)$ and $af_\pi(\infty)$, only. The leading order expressions are able to describe the data at $\beta = 5.29$, $\kappa = 0.13632$ on all three volumes, which include data with $m_\pi L < 3$ as well as $m_\pi L > 4$. This gives us confidence that the fits provide a reasonable infinite volume extrapolation at the lighter mass point as well, where we do not have access to data with larger $m_\pi L$.[2] All fits gave $\chi^2/\text{d.o.f.} < 1.4$.

To obtain continuum numbers, we need to renormalize the axial vector current. The latter reads

$$\mathcal{A}_\mu^R = Z_A(1 + b_A a m_q)\mathcal{A}_\mu. \tag{8}$$

The coefficient b_A is required to maintain $O(a)$ improvement for nonvanishing quark masses m_q as well. The renormalization constant Z_A has been computed nonperturbatively in [7], employing the Rome–Southampton method [6], with the result

β	5.25	5.29	5.40
Z_A	0.760(1)	0.764(1)	0.777(1)

(9)

The coefficient b_A is only known perturbatively [23],

$$b_A = 1 + 0.1522 g^2. \tag{10}$$

In Table 2 we give g_A^R in the infinite volume. For pion masses $m_\pi \leqslant 300$ MeV we demand that we have at least two lattice volumes to ensure a controlled extrapolation. For this reason we excluded the point at $\beta = 5.25$, $\kappa = 0.13620$ from the analysis.

Our results for g_A^R are plotted in Fig. 7. Since after finite volume corrections the lightest pion mass is 130 MeV, no extrapolation is required. At the lightest pion mass we find

$$g_A^R = 1.24 \pm 0.04, \tag{11}$$

in good agreement with the previous determination and the experimental value. It turns out that g_A^R hovers around ≈ 1.1 for $m_\pi \gtrsim 250$ MeV, a feature it shares with most other lattice calculations [5]. Only within the last 100 MeV from the physical point does g_A^R rise to its final value. This phenomenon is not totally unexpected, from general arguments [24] and from ChEFT [10,20,25]. Near the chiral limit ChEFT predicts, following [10],

$$\begin{aligned} g_A^R(m_\pi) = g_A^0 &- \frac{g_A^{0\,3}}{16\pi^2 f_0^2} m_\pi^2 \\ &+ 4\big[B_9^r(m_{\pi\,\text{phys}}) - 2g_A^0 B_{20}^r(m_{\pi\,\text{phys}})\big]m_\pi^2 \\ &- \frac{g_A^{0\,3} + g_A^0/2}{4\pi^2 f_0^2} m_\pi^2 \ln(m_\pi/m_{\pi\,\text{phys}}) + O\big(m_\pi^3\big). \end{aligned} \tag{12}$$

To this order, both sets of chiral expansions, [10,20] and [25], are equivalent with $B_9 = d_{16}$ and $B_{20} = d_{28}$. In (12) we have chosen $\lambda = m_{\pi\,\text{phys}}$ (λ being the scale parameter of the dimensional regularization). The coupling B_9^r cannot be observed independent of B_{20}^r. Taking $B_{20}^r(m_{\pi\,\text{phys}}) \equiv 0$, the preferred value is [26] $B_9^r(m_{\pi\,\text{phys}}) = (-1.4 \pm 1.2)\ \text{GeV}^{-2}$. A fit of the leading order chiral formula (12) to the data points in Fig. 7 is shown by the shaded area. The fit gives $g_A^0 = 1.26(7)$ and $B_9^r(m_{\pi\,\text{phys}}) = (-2.1 \pm 1.0)\ \text{GeV}^{-2}$.

Our results for f_π^R are plotted in Fig. 8. Again, no extrapolation to the physical point is needed. At the lightest pion mass we find

$$f_\pi^R = 89.7 \pm 1.5 \pm 1.8\ \text{MeV}, \tag{13}$$

using $r_0 = 0.50(1)$ fm. The second error in Eq. (13) is due to the error on r_0.

Instead of taking f_π^R at the lowest pion mass, Eq. (13), it might be a better idea to include the adjacent data points in the analysis as well and fit the data by a chiral ansatz [19],

[2] It should be noted though that $m_\pi L$ is not the ultimate benchmark, contrary to common belief. With decreasing pion mass the corrections turn into a $1/L^3$ behavior. See also [22].

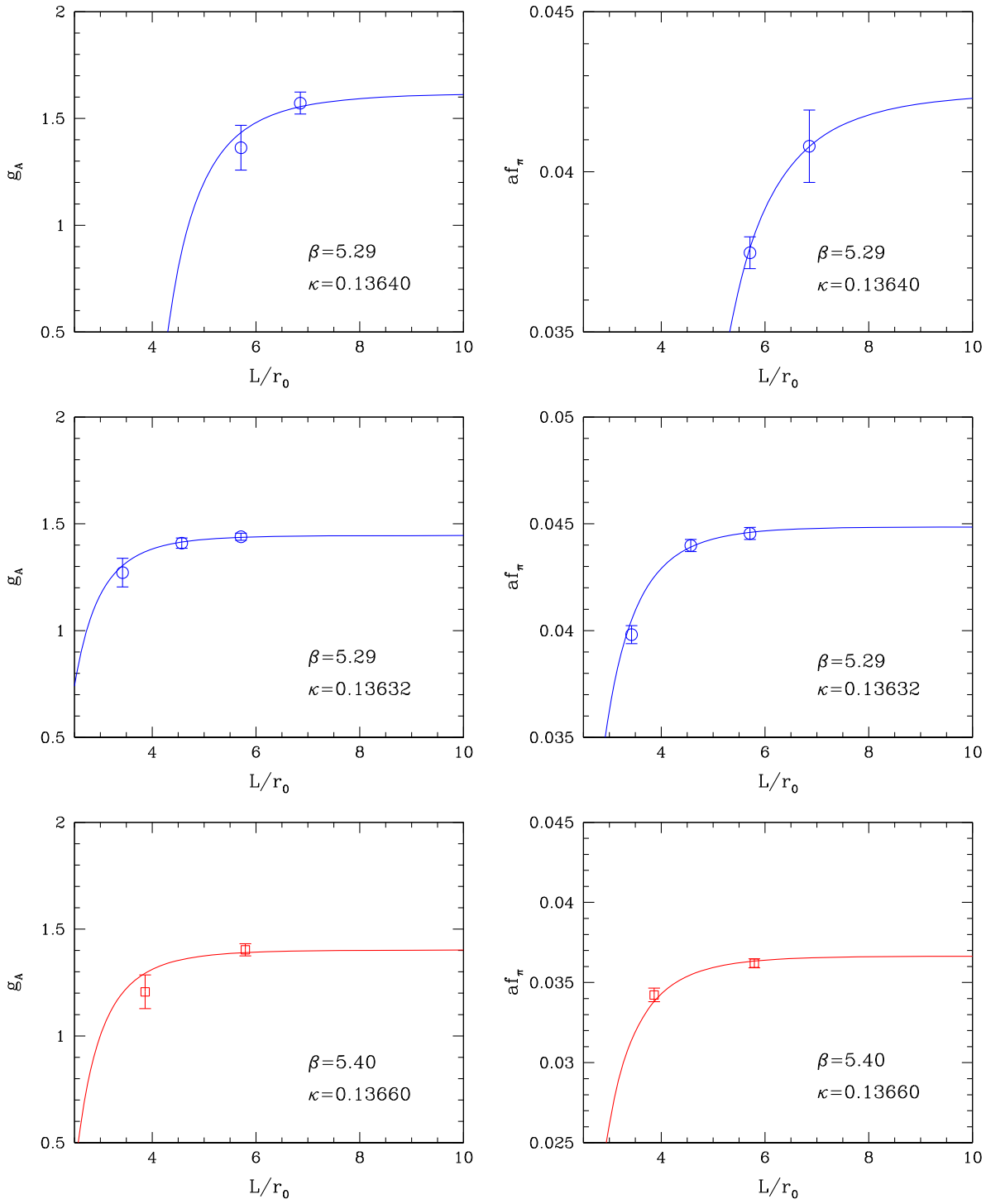

Fig. 6. The bare axial charge g_A and the bare pion decay constant af_π as a function of the spatial extent of the lattice, together with the leading order finite size corrections of Eqs. (19) and (20).

$$f_\pi^R = f_0\left[1 - \frac{m_\pi^2}{16\pi^2 f_\pi^{R2}} \ln\left(\Lambda_4^2/m_\pi^2\right)\right]^{-1} + A\, m_\pi^4. \tag{14}$$

The result of the fit is shown in Fig. 8. At the physical point we obtain

$$f_\pi^R = 89.6 \pm 1.1 \pm 1.8 \text{ MeV}, \tag{15}$$

in full agreement with the result (13). The main effect is that the statistical error has reduced by 30%. In the chiral limit we obtain $f_0 = 86(1)$ MeV, which agrees with the assumption made in Section 3.2. A fit of the chiral ansatz (14) to the lowest four data points with $A = 0$ gives the low-energy constant

$$\bar{l}_4 = \ln\left(\Lambda_4^2/m_{\pi\,\text{phys}}^2\right) = 4.2 \pm 0.1. \tag{16}$$

4. Conclusions

We have successfully computed the nucleon axial charge and the pion decay constant in $N_f = 2$ lattice QCD with nonpertur-

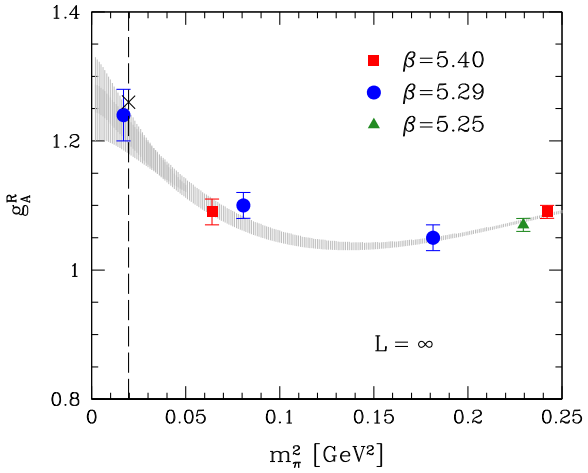

Fig. 7. The renormalized axial charge g_A^R in the infinite volume plotted against $m_\pi^2(\infty)$, together with the experimental value $g_A = 1.27$ (×). The shaded area shows the fit of Eq. (12) to the data.

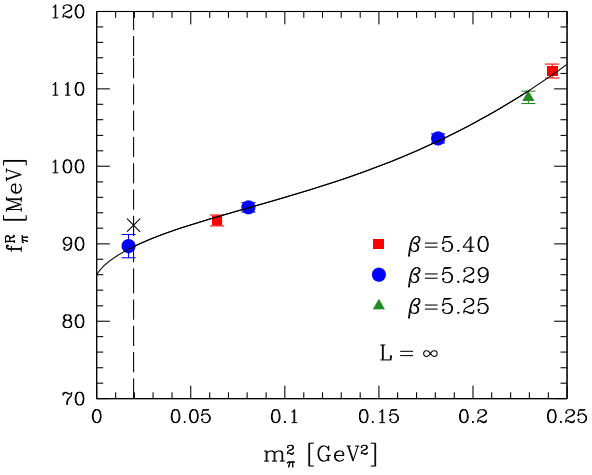

Fig. 8. The renormalized pion decay constant f_π^R in the infinite volume plotted against $m_\pi^2(\infty)$, together with the experimental value $f_\pi = 92.2$ MeV (×). The curve shows a fit of Eq. (14) to the data.

batively $O(a)$ improved Wilson fermions. A novel feature of our calculations is that we have data at virtually physical pion mass and for a variety of lattice volumes and spacings at our disposal. While our simulations at different lattice spacings indicate that our results are free from discretization effects, simulations on different lattice volumes indicate the presence of large finite size effects. Two approaches have been pursued.

The main result of this Letter is a determination of g_A^R from the ratio g_A/f_π, which is free of finite size effects and renormalization errors. We found that this ratio has a smooth behavior as a function of quark mass, and can be essentially described by a polynomial in m_π^2, leading to $g_A^R = 1.29(5)(3)$ at the physical point, in excellent agreement with experiment. Here we have used $r_0 = 0.50(1)$ fm to set the scale, which we obtained from fits to the nucleon mass [13]. This result is in perfect agreement with ALPHA [28], who finds $r_0 = 0.503(10)$ fm using f_K to set the scale and the same action. In contrast, ETM finds consistently lower values of r_0, $r_0 = 0.465(6)(14)$ fm from the nucleon mass [29] and $r_0 = 0.420(9)(+10/-11)$ fm from using f_π to set the scale [30]. If correct, this would raise our number for g_A accordingly.

We attempted a direct calculation of g_A^R and f_π^R, taking account of finite size corrections and renormalization. To our knowledge, this is the first time finite size corrections have been applied to g_A at physical pion masses. Both approaches give consistent results, suggesting that finite size corrections to both g_A and f_π are well described by ChEFT and ChPT.

Acknowledgements

The gauge configurations were generated using the BQCD code [35] on the BlueGene/L and BlueGene/P at NIC (Jülich), the BlueGene/L at EPCC (Edinburgh), the SGI ICE 8200 at HLRN (Berlin and Hannover), and on QPACE. The Chroma software library [36] was used in the data analysis. This work would not have been possible without the input of Dirk Pleiter. We thank him most sincerely for his contributions. Benjamin Gläßle computed some two- and three-point functions for us, which we gratefully acknowledge. This work has been supported partly by the European Commission grants 283286 (HadronPhysics3) and 227431 (HadronPhysics2), and by the DFG under contract SFB/TR 55 (Hadron Physics from Lattice QCD). J.M.Z. is supported by the Australian Research Council grant FT100100005. We thank all funding agencies.

Appendix A. Finite size corrections

Let us first consider g_A. Utilizing the (nonrelativistic) small scale expansion (SSE) of the ChEFT, including pion, nucleon (N) and $\Delta(1232)$ degrees of freedom, we obtain to $O(\epsilon^3)$ [10]

$$\frac{g_A(L) - g_A(\infty)}{g_A(\infty)} = -\frac{m_\pi^2}{4\pi^2 f_0^2} \sum_{\boldsymbol{n}\neq 0} \frac{K_1(\lambda|\boldsymbol{n}|)}{\lambda|\boldsymbol{n}|} + \Delta(L) \tag{17}$$

with

$$\begin{aligned}
\Delta(L) = {} & \frac{g_A^2 m_\pi^2}{6\pi^2 f_0^2} \sum_{\boldsymbol{n}\neq 0} \left[K_0(\lambda|\boldsymbol{n}|) - \frac{K_1(\lambda|\boldsymbol{n}|)}{\lambda|\boldsymbol{n}|} \right] \\
& + \frac{25 c_A^2 g_1}{81\pi^2 g_A f_0^2} \int_0^\infty dy\, y \\
& \times \sum_{\boldsymbol{n}\neq 0} \left[K_0\big(\lambda(y)|\boldsymbol{n}|\big) - \frac{\lambda(y)|\boldsymbol{n}|}{3} K_1\big(\lambda(y)|\boldsymbol{n}|\big) \right] \\
& - \frac{c_A^2}{\pi^2 f_0^2} \int_0^\infty dy\, y \\
& \times \sum_{\boldsymbol{n}\neq 0} \left[K_0\big(\lambda(y)|\boldsymbol{n}|\big) - \frac{\lambda(y)|\boldsymbol{n}|}{3} K_1\big(\lambda(y)|\boldsymbol{n}|\big) \right] \\
& + \frac{8 c_A^2 m_\pi^2}{27\pi^2 f_0^2 \Delta_0} \int_0^\infty dy \\
& \times \sum_{\boldsymbol{n}\neq 0} \left(\frac{\lambda(y)}{\lambda} \right)^2 \left[K_0\big(\lambda(y)|\boldsymbol{n}|\big) - \frac{K_1(\lambda(y)|\boldsymbol{n}|)}{\lambda(y)|\boldsymbol{n}|} \right] \\
& - \frac{4 c_A^2 m_\pi^3}{27\pi f_0^2 \Delta_0} \sum_{\boldsymbol{n}\neq 0} \frac{e^{-\lambda|\boldsymbol{n}|}}{\lambda|\boldsymbol{n}|},
\end{aligned} \tag{18}$$

where $\lambda = m_\pi L$ and $\lambda(y) = f(m_\pi, y)L$ with $f(m_\pi, y) = \sqrt{m_\pi^2 + y^2 + 2y\Delta_0}$, Δ_0 being the Δ–N mass difference. K_0 and

K_1 denote the modified Bessel functions, and c_A and g_1 are the leading axial ΔN and $\Delta\Delta$ couplings. The parameter c_A should not be confused with the improvement coefficient c_A in Eq. (1).

The second term in Eq. (17), $\Delta(L)$, receives contributions from chiral loops, which renormalize the axial charge and act on intermediate Δ baryons [10]. It turns out that the various contributions to $\Delta(L)$ effectively cancel each other over a wide range of λ values. This has been noticed by the authors of [27] as well. To state an example, let us consider the $48^3 \times 64$ lattice at $\beta = 5.29$, $\kappa = 0.13640$. This lattice has the lowest pion mass and is especially important for our final conclusions. Taking $c_A = 1.5$ from [31] and $g_1 = 2.16$ from $SU(6)$, we find -0.044 for the total contribution, but only $+0.001$ for $\Delta(L)$. We thus may assume

$$\frac{g_A(L) - g_A(\infty)}{g_A(\infty)} = -\frac{m_\pi^2}{4\pi^2 f_0^2} \sum_{\substack{\boldsymbol{n} \\ |\boldsymbol{n}|\neq 0}} \frac{K_1(\lambda|\boldsymbol{n}|)}{\lambda|\boldsymbol{n}|}. \tag{19}$$

The finite size corrections to f_π have been computed in [11] within the context of ChPT. To NLO ($\propto m_\pi^2$) the outcome is

$$\frac{f_\pi(L) - f_\pi(\infty)}{f_\pi(\infty)} = -\frac{m_\pi^2}{4\pi^2 f_0^2} \sum_{\substack{\boldsymbol{n} \\ |\boldsymbol{n}|\neq 0}} \frac{K_1(\lambda|\boldsymbol{n}|)}{\lambda|\boldsymbol{n}|}. \tag{20}$$

The NNLO corrections are found to be very small on our configurations and, thus, can safely be neglected.

The investigations above show that the leading finite size corrections to g_A and f_π, Eqs. (19) and (20), are identical. Once f_0, the pion decay constant in the chiral limit, has been fixed, expressions (19) and (20) have only one free parameter, $g_A(\infty)$ and $f_\pi(\infty)$, respectively.

The NLO correction to the pion mass reads [11]

$$\frac{m_\pi(L) - m_\pi(\infty)}{m_\pi(\infty)} = \frac{m_\pi^2}{16\pi^2 f_0^2} \sum_{\substack{\boldsymbol{n} \\ |\boldsymbol{n}|\neq 0}} \frac{K_1(\lambda|\boldsymbol{n}|)}{\lambda|\boldsymbol{n}|}. \tag{21}$$

At smaller values of $m_\pi L$, $m_\pi L \lesssim 3$, this expression alone cannot describe the observed finite size effects [13]. That is not surprising, since in a finite spatial box chiral symmetry does not break down spontaneously. This is because giving the system enough time it will rotate through all vacua. This results in a mass gap at vanishing quark masses [32–34],

$$m_{\pi\,\mathrm{res}} = \frac{3}{2 f_0^2 L^3 (1+\Delta)} \tag{22}$$

with

$$\Delta = \frac{2}{f_0^2 L^2} 0.2257849591 + \frac{1}{f_0^4 L^4}\Bigg[0.088431628 - \frac{0.8375369106}{3\pi^2}\left(\frac{1}{4}\ln\left(\Lambda_1^2 L^2\right) + \ln\left(\Lambda_2^2 L^2\right)\right)\Bigg], \tag{23}$$

where Λ_i are the intrinsic scale parameters of the low-energy constants $\bar{l}_i = \ln(\Lambda_i^2/m^2_{\pi\,\mathrm{phys}})$ [19], with $m_{\pi\,\mathrm{phys}}$ being the physical pion mass. In [22] we found that the pion mass extrapolates indeed to a finite value in the chiral limit, in good agreement with the expected result (22). This also has an effect on m_π in the region of small, but nonvanishing, quark masses [22]. We thus expect the finite size correction to be effectively given by

$$m_\pi(L) = m_\pi(\infty) + \frac{m_\pi^3}{16\pi^2 f_0^2} \sum_{\substack{\boldsymbol{n} \\ |\boldsymbol{n}|\neq 0}} \frac{K_1(\lambda|\boldsymbol{n}|)}{\lambda|\boldsymbol{n}|} + \frac{3c(m_\pi)}{2 f_0^2 L^3 (1+\Delta)} \tag{24}$$

with the parameter $c(m_\pi)$ rapidly dropping to zero at larger pion masses.

References

[1] R.G. Edwards, G.T. Fleming, Ph. Hägler, J.W. Negele, K. Orginos, A.V. Pochinsky, D.B. Renner, D.G. Richards, W. Schroers, Phys. Rev. Lett. 96 (2006) 052001, arXiv:hep-lat/0510062.
[2] T. Yamazaki, Y. Aoki, T. Blum, H.-W. Lin, M.-F. Lin, S. Ohta, S. Sasaki, R.J. Tweedie, J.M. Zanotti, Phys. Rev. Lett. 100 (2008) 171602, arXiv:0801.4016 [hep-lat].
[3] C. Alexandrou, M. Brinet, J. Carbonell, M. Constantinou, P.A. Harraud, P. Guichon, K. Jansen, T. Korzec, M. Papinutto, Phys. Rev. D 83 (2011) 045010, arXiv:1012.0857 [hep-lat].
[4] S. Capitani, M. Della Morte, G. von Hippel, B. Jäger, A. Jüttner, B. Knippschild, H.B. Meyer, H. Wittig, Phys. Rev. D 86 (2012) 074502, arXiv:1205.0180 [hep-lat].
[5] For reviews see H.-W. Lin, arXiv:1112.2435 [hep-lat];
H.-W. Lin, PoS LATTICE 2012 (2012) 013, arXiv:1212.6849 [hep-lat].
[6] G. Martinelli, C. Pittori, C.T. Sachrajda, M. Testa, A. Vladikas, Nucl. Phys. B 445 (1995) 81, arXiv:hep-lat/9411010;
M. Göckeler, R. Horsley, H. Oelrich, H. Perlt, D. Petters, P.E.L. Rakow, A. Schäfer, G. Schierholz, A. Schiller, Nucl. Phys. B 544 (1999) 699, arXiv:hep-lat/9807044.
[7] M. Göckeler, R. Horsley, Y. Nakamura, H. Perlt, D. Pleiter, P.E.L. Rakow, A. Schäfer, G. Schierholz, A. Schiller, H. Stüben, J.M. Zanotti, Phys. Rev. D 82 (2010) 114511, arXiv:1003.5756 [hep-lat].
[8] M. Constantinou, M. Costa, M. Göckeler, R. Horsley, H. Panagopoulos, H. Perlt, P.E.L. Rakow, G. Schierholz, A. Schiller, PoS LATTICE 2012 (2012) 239, arXiv:1210.7737 [hep-lat].
[9] S.R. Beane, M.J. Savage, Phys. Rev. D 70 (2004) 074029, arXiv:hep-ph/0404131.
[10] A. Ali Khan, M. Göckeler, P. Hägler, T.R. Hemmert, R. Horsley, D. Pleiter, P.E.L. Rakow, A. Schäfer, G. Schierholz, T. Wollenweber, J.M. Zanotti, Phys. Rev. D 74 (2006) 094508, arXiv:hep-lat/0603028.
[11] G. Colangelo, S. Dürr, C. Haefeli, Nucl. Phys. B 721 (2005) 136, arXiv:hep-lat/0503014.
[12] S. Collins, M. Göckeler, Ph. Hägler, T. Hemmert, R. Horsley, Y. Nakamura, A. Nobile, H. Perlt, D. Pleiter, P.E.L. Rakow, A. Schäfer, G. Schierholz, A. Sternbeck, H. Stüben, F. Winter, J.M. Zanotti, PoS LATTICE 2010 (2010) 153, arXiv:1101.2326 [hep-lat].
[13] G.S. Bali, P.C. Bruns, S. Collins, M. Deka, B. Gläßle, M. Göckeler, L. Greil, T.R. Hemmert, R. Horsley, J. Najjar, Y. Nakamura, A. Nobile, D. Pleiter, P.E.L. Rakow, A. Schäfer, R. Schiel, G. Schierholz, A. Sternbeck, J.M. Zanotti, Nucl. Phys. B 866 (2013) 1, arXiv:1206.7034 [hep-lat].
[14] M. Della Morte, R. Hoffmann, R. Sommer, J. High Energy Phys. 0503 (2005) 029, arXiv:hep-lat/0503003.
[15] M. Göckeler, R. Horsley, E.-M. Ilgenfritz, H. Perlt, P.E.L. Rakow, G. Schierholz, A. Schiller, Phys. Rev. D 53 (1996) 2317, arXiv:hep-lat/9508004.
[16] S. Capitani, M. Göckeler, R. Horsley, B. Klaus, H. Oelrich, H. Perlt, D. Petters, D. Pleiter, P.E.L. Rakow, G. Schierholz, A. Schiller, P. Stephenson, Nucl. Phys. B, Proc. Suppl. 73 (1999) 294, arXiv:hep-lat/9809172.
[17] B.J. Owen, J. Dragos, W. Kamleh, D.B. Leinweber, M.S. Mahbub, B.J. Menadue, J.M. Zanotti, arXiv:1212.4668 [hep-lat].
[18] M. Göckeler, R. Horsley, D. Pleiter, P.E.L. Rakow, G. Schierholz, W. Schroers, H. Stüben, J.M. Zanotti, PoS LAT 2006 (2006) 063, arXiv:hep-lat/0509196, 2005.
[19] G. Colangelo, J. Gasser, H. Leutwyler, Nucl. Phys. B 603 (2001) 125, arXiv:hep-ph/0103088.
[20] M. Procura, B.U. Musch, T.R. Hemmert, W. Weise, Phys. Rev. D 75 (2007) 014503, arXiv:hep-lat/0610105.
[21] G. Colangelo, S. Dürr, Eur. Phys. J. C 33 (2004) 543, arXiv:hep-lat/0311023.
[22] W. Bietenholz, M. Göckeler, R. Horsley, Y. Nakamura, D. Pleiter, P.E.L. Rakow, G. Schierholz, J.M. Zanotti, Phys. Lett. B 687 (2010) 410, arXiv:1002.1696 [hep-lat].
[23] S. Sint, P. Weisz, Nucl. Phys. B 502 (1997) 251, arXiv:hep-lat/9704001.
[24] R.L. Jaffe, Phys. Lett. B 529 (2002) 105, arXiv:hep-ph/0108015.
[25] V. Bernard, U.-G. Meissner, Phys. Lett. B 639 (2006) 278, arXiv:hep-lat/0605010.
[26] T.R. Hemmert, M. Procura, W. Weise, Phys. Rev. D 68 (2003) 075009, arXiv:hep-lat/0303002.
[27] N.L. Hall, A.W. Thomas, R.D. Young, J.M. Zanotti, arXiv:1205.1608 [hep-lat].
[28] P. Fritzsch, F. Knechtli, B. Leder, M. Marinkovic, S. Schaefer, R. Sommer, F. Virotta, Nucl. Phys. B 865 (2012) 397, arXiv:1205.5380 [hep-lat].
[29] C. Alexandrou, R. Baron, J. Carbonell, V. Drach, P. Guichon, K. Jansen, T. Korzec, O. Pène, Phys. Rev. D 80 (2009) 114503, arXiv:0910.2419 [hep-lat].

[30] R. Baron, Ph. Boucaud, P. Dimopoulos, F. Farchioni, R. Frezzotti, V. Gimenez, G. Herdoiza, K. Jansen, V. Lubicz, C. Michael, G. Münster, D. Palao, G.C. Rossi, L. Scorzato, A. Shindler, S. Simula, T. Sudmann, C. Urbach, U. Wenger, J. High Energy Phys. 1008 (2010) 097, arXiv:0911.5061 [hep-lat].
[31] T.A. Gail, T.R. Hemmert, Eur. Phys. J. A 28 (2006) 91, arXiv:nucl-th/0512082.
[32] H. Leutwyler, Phys. Lett. B 189 (1987) 197.
[33] P. Hasenfratz, F. Niedermayer, Z. Phys. B 92 (1993) 91, arXiv:hep-lat/9212022.
[34] P. Hasenfratz, Nucl. Phys. B 828 (2010) 201, arXiv:0909.3419 [hep-th].
[35] Y. Nakamura, H. Stüben, PoS LATTICE 2010 (2010) 040, arXiv:1011.0199 [hep-lat].
[36] R.G. Edwards, B. Joó, Nucl. Phys. B, Proc. Suppl. 140 (2005) 832, arXiv:hep-lat/0409003.